# Rigidity Coefficients of Rubber Belts for Dynamic Testing of Modulus of Elasticity and Shear Modulus of Non-wood Engineered Board

Benhuan Xu,<sup>a</sup> Qiyun Xu,<sup>a</sup> Zheng Wang,<sup>a,\*</sup> Zhaoyu Shen,<sup>a</sup> and Qing Lin <sup>b</sup>

To determine the appropriate stiffness coefficient k values for rubber belts used in dynamic testing of the elastic modulus and shear modulus of timber and solid wood composite materials, this study employed three different thicknesses of rubber belts. Dynamic tests were conducted on straw boards, Laminated Veneer Lumber (LVL), and Spruce-Pine-Fir (SPF) materials, and the results were validated and analyzed using static four-point bending tests. The conclusions drawn from this research indicate that the range of stiffness coefficient k values for the rubber belts obtained through dynamic testing fell between 0.05 and 0.28 N/m. The correctness of the dynamic testing method was verified through static four-point bending tests. The error levels for elastic modulus E and shear modulus E of the same type of board measured using the three different rubber belts were below 9.5% and 9.8%, respectively.

DOI: 10.15376/biores.19.4.8512-8526

Keywords: Wood; Rubber belts; Stiffness coefficient; Transient excitation method; Four-point bending method

Contact information: a: College of Materials Science and Engineering, Nanjing Forestry University, Nanjing, 210037, China; b: Department of Physical Education, Nanjing Forestry University, Nanjing, 210037, China; \*Corresponding author: wangzheng63258@163.com

### INTRODUCTION

Wood has been a major building material since ancient times because it is easy to obtain and process. With the rapid development of the national economy and the increasing improvement of people's living standards, users have put forward higher requirements for the quantity and quality of wood and its products. Especially in recent decades, the world's focus on wood resources has gradually shifted from natural forests (Yin 1996). This shift presents a series of new research challenges for scientists of wood industry (Mei *et al.* 2005). A key feature of solid wood composites is that they not only maintain the respective characteristics of the original single-component materials but also complement each other's performance. This results in materials with excellent overall performance, leading to their wide use in the fields of aviation, aerospace, automotive, and sporting goods. At the same time, the use of artificial fast-growing forest wood and other materials into new wood composite materials is an effective way to alleviate the scarcity of wood resources and enhance the structure of the wood industry.

The elastic constant of wood is an important mechanical property parameter, which reflects its ability to resist deformation under the action of external forces. There are two main types of methods for testing the elastic constants of wood: static and dynamic methods. Among them, the dynamic test method has proven to be a common and successful

method due to its advantages of speed, simplicity, and high reliability; in addition, its results are in good agreement with those of the traditional static method (Wang *et al.* 2014; Hu *et al.* 2015; Wang *et al.* 2015; Wang *et al.* 2018). Additionally, many studies use probabilistic methods to study the mechanical properties of materials (Peng *et al.* 2018; Wang and Ghanem 2021; Wang and Ghanem 2022; Liu *et al.* 2023a; Wang and Ghanem 2023a; Wang *et al.* 2023). Some use structural design to study the mechanical properties of materials (ASTM D3044-16 2016; Wang *et al.* 2016; Wang *et al.* 2019; Dauletbek *et al.* 2021; Su *et al.* 2021; Zhou *et al.* 2021; Quintero *et al.* 2022; Wang and Ghanem 2023b).

When the elastic modulus and shear modulus of wood and its solid wood composite materials are measured by the free board specimen, the rigidity coefficient k of the rubber belt used for suspension has a great influence on the test results, which is seldom studied in the test. The motivation for choosing rubber belts over rigid steel surfaces may be to minimize damage to the wood samples and replicate more realistic testing conditions. Using rigid steel surfaces could exert excessive pressure, potentially damaging the wood samples and thereby compromising the accuracy of the test results. Meanwhile, it may lead to uneven load distribution, which in turn affects the measurement accuracy of elastic modulus and shear modulus (Liu et al. 2023b). Therefore, to give the suitable range of the stiffness coefficient k of the rubber belts, the test was conducted using three thicknesses of rubber belts for dynamic testing of the elastic and shear modulus of freeboard straw board, laminated veneer lumber (LVL), and spruce-pine-fir (SPF) materials, and its static symmetric four-point bending method and asymmetric four-point bending method were verified and analyzed to give the suitable range of the stiffness coefficient k of the rubber belts, with a view to the dynamic testing of the wood freeboard elastic and shear modulus. It is expected to provide useful technical support for the accuracy and reliability of dynamic testing of the modulus of elasticity and shear modulus of wood freeboard.

## **EXPERIMENTAL**

#### **Materials**

In this paper, three materials, straw board, LVL, and SPF, all made in China, were selected. The dimensional parameters of each board are summarized in Table 1. Figure 1 shows a schematic diagram of the longitudinal and transverse specimens under the straw board, whose whole board length direction is longitudinal (x-direction) and width direction is transverse (y-direction). In Fig. 1,  $62 \times 7$  indicates that the width of the straw board specimen is 62 mm and the number of specimens is 7. When producing strawboard, the straw particles are typically aligned along one primary direction, often referred to as the "machine direction" or "longitudinal direction," akin to oriented strand board (OSB). Specimens were derived from the entire boards of both straw board and LVL board materials. For the straw board, samples were cut longitudinally (in the x-direction) to create JZ specimens, and transversely (in the y-direction) to create JH specimens. Similarly, the LVL board provided longitudinal LH specimens along the x-direction and transverse LZ specimens along the y-direction.

Figure 2 shows a schematic diagram of the chordal specimen of SPF plate. Because the SPF plate is a specification material with limited size, only the chordal specimen of SPF plate is taken. The length direction of the chord of the SPF board is the longitudinal direction (*x*-direction), and the vertical arrangement is the transverse direction (*y*-

direction). Specimens designated as S were crafted using materials sliced along the chord of the SPF board.

late

Name	Direction	Size Specification (mm × mm × mm)	Number	Quantity (Block)
Ctrow Board	Transverse	420 × 62 × 18	JH	7
Straw Board	Longitudinal	420 × 62 × 18	JZ	7
LV/L Diete	Transverse	384 × 48 × 16	LH	5
LVL Plate	Longitudinal	384 × 48 × 16	LZ	5
SPF Board	Chordwise	384 × 48 × 16	S	5

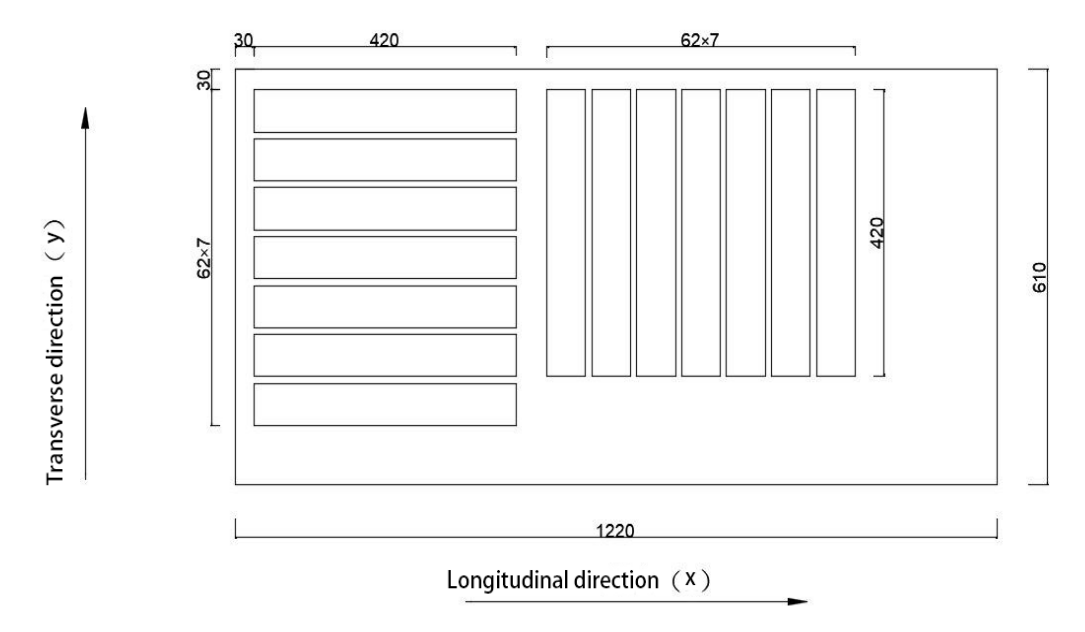
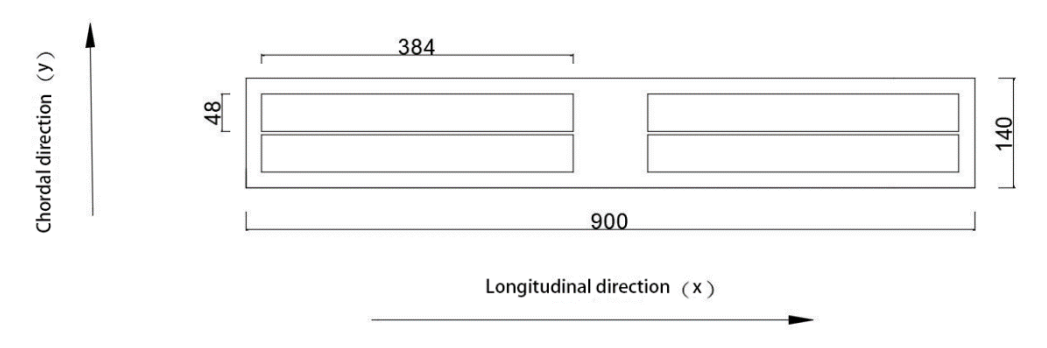


Fig. 1. Schematic of the longitudinal and transverse specimens under the straw board (Unit: mm)



**Fig. 2.** Illustration of SPF plate chordal specimen undercut (Unit: mm; Plate thickness 38 mm, made in China)

## **Test Instruments and Accessories**

The CRAS vibration and dynamic signal acquisition and analysis system comprise one set, which includes a signal conditioning box, a signal acquisition box, and SsCras analysis software (developed by Anzheng Fashion Group Co., Ltd., with a specified version v7.4, originating from Nanjing, China), along with its dedicated computer.

Additionally, the set includes the following equipment: one CA-YD-125 voltage acceleration sensor with a mass of 1.5 g and a sensitivity of 0.089 pc/m·s<sup>-2</sup>, one BE120-5 AA type strain gauge with a sensitivity coefficient of 2.11% and a strain grid length of 5 mm  $\times$  2.8 mm, one rubber force hammer, one JY501 electronic balance with an accuracy of 0.1 g, one vernier caliper with a precision of 0.02 mm, one steel ruler ranging from 0 to 500 mm, and one HK-30 inductive wood moisture tester.

There were three types of rubber belts (Wang *et al.* 2015) (short loops made of rubber and latex). Fine rubber belts, with a 1.5 mm thickness; medium rubber belts, with a 4.5 mm thickness, and coarse rubber belts, with a 15 mm thickness.

#### Methods

Free board transient excitation method

According to the transverse bending theory of Eulerian beams, the first-order bending frequency of a free beam is related to the dynamic elastic modulus E as Eq. 1,

$$E = 0.9462\rho l^4 \frac{f_{1b}^2}{h^2} \tag{1}$$

where E is dynamic measurement of the elastic modulus of the specimen (Pa),  $\rho$  is air-dry density (kg/m<sup>3</sup>),  $f_{1b}$  is the first-order bending frequency value (Hz), l is the length of the beam (m), and h is the thickness of the beam (m).

The free board vibration coefficient  $\gamma$  in the freeboard torsional vibration method is used to calculate the freeboard of straw board, LVL board, and SPF board. The relationship between the first-order torsion frequency of the free-plate and the shear modulus is given by Eq. 2,

$$G = \frac{\pi^2 \rho(l/2)^2 b^2 f_{1t}^2}{\gamma \beta h^2} (l/b = 1 \sim 8)$$
 (2)

where G is the specimen shear modulus (Pa), l is the freeboard length (m), b is the freeboard width (m), h is the freeboard thickness (m),  $f_{1t}$  is the freeboard first-order torsion frequency (Hz);  $\rho$  is air dry density (kg/m³);  $\gamma$  is the freeboard vibrational form factor, and  $\beta = \frac{1}{16} \left[ \frac{16}{3} - 3.36 \frac{h}{b} \left( 1 - \frac{h^4}{12b^4} \right) \right]$ .

The equations for the vibration shape coefficient  $\gamma$  of this straw board, LVL board, and SPF board free board specimen are as follows:

**Longitudinal direction:** 
$$\gamma = 7.4539(1 - 0.1187 \frac{b}{l} + 0.6013 \frac{b^2}{l^2} - 0.3824 \frac{b^3}{l^3})$$

Correlation coefficient  $\gamma = 0.99998$ , n = 6;

Transverse direction: 
$$\gamma = 7.4119(1 - 0.0184 \frac{b}{l} + 0.0565 \frac{b^2}{l^2} - 0.1023 \frac{b^3}{l^3})$$
  
Correlation coefficient  $\gamma = 0.99998$ ,  $n = 6$ 

The relationship between the stiffness coefficient k of its free-plate rubber belt and its inherent frequency is given by Eq. 3 (Zhang 2015),

$$k = m \times (2\pi f)^2 \tag{3}$$

where k is the rigidity coefficient of the rubber belt (N/m), m is the mass of the specimen (kg), and f is the value of the inherent frequency of the rubber belt (Hz).

The free board transient excitation method was used to dynamically test the elastic modulus E and shear modulus G of straw, LVL, and SPF plates. A total of 0.224 L and 0.776 L (where L represents the length of the specimen) from one end of the plate specimen

were suspended with rubber belts to realize the free board restraint method, and the accelerometer was fixed at the corner point of the plate to connect to the CRAS vibration and dynamic signal acquisition and analysis system and its SsCras signal analysis software, as shown in Fig. 3. Free vibration of the plate was generated by hammering the corner points of the specimen, and vibration signals were received by the accelerometer and converted into electrical signals for output. The electrical signal is amplified and filtered by the signal conditioning instrument and input to the collection box. The spectrum of the specimen is converted by A/D. At this time, the first-order bending frequency  $f_{1b}$  and first-order torsional frequency  $f_{1t}$  of the specimen can be obtained from the spectrum, and their frequency values can be substituted into Eqs. 1 and 2 to calculate E and G of the specimen.

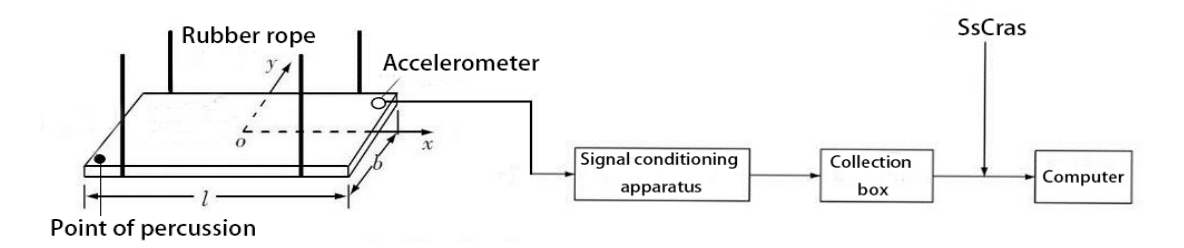


Fig. 3. Block diagram of free board transient excitation method test

Symmetric four-point bending method

The mechanical model for the static calculation of the symmetrical four-point bending beam is shown in Fig. 4. The results of ANSYS static analysis (AdCras, Anzheng Fashion Group Co., Ltd., v.7.4, Nanjing, China) show that there is no point where the transverse stress (along the width of the beam) is equal to zero on the upper and lower surfaces of the beam in this section.

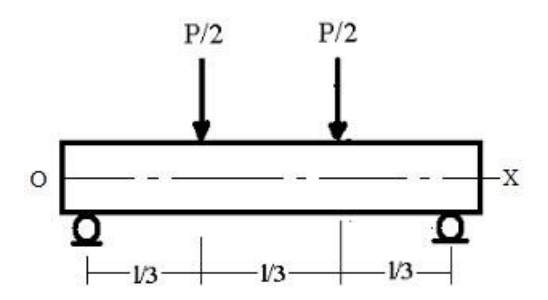


Fig. 4. Schematic diagram of symmetrical four-point bending beam loading

Normal stress at each point on the upper and lower surfaces of a symmetrical four-point bending beam (1/3-1/3 loading) in the pure bending section is calculated using Eq. 4.

$$\sigma = \frac{Pl}{hh^2} \tag{4}$$

If the longitudinal strain at the center of the upper and lower surfaces of the beam is according to Hooke's law, its modulus of elasticity E can be tabulated as  $E = \frac{Pl}{bh^2 \varepsilon_x}$ , and it can be written in an incremental form, as Eq. 5, that is easy to test:

$$E = \frac{\Delta P \cdot l}{b h^2 \Delta \varepsilon_X} \tag{5}$$

In this expression, E is the modulus of elasticity (MPa), l is the beam length (mm), b is the beam width (mm), h is the beam thickness (mm),  $\Delta P$  is the load increment (N), and  $\Delta \varepsilon_{\chi}$  is longitudinal strain increment.

A  $0^{\circ}$  (transverse) strain gauge was placed at the center points of the upper and lower surfaces of the beam specimen (Fig. 5). A symmetrical four-point bending load was applied to the beam (Fig. 4), and the longitudinal and transverse strains at the center point C were measured. The strain measurements each occupy one channel of the strain gauge. The  $0^{\circ}$  gauges on the upper and lower surfaces are connected by the half-bridge method.

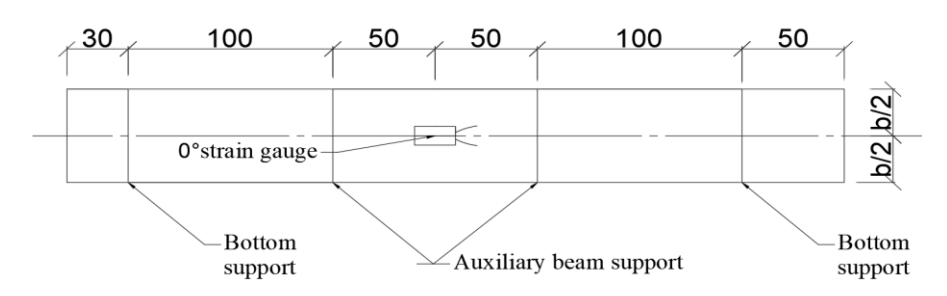


Fig. 5. Schematic of symmetrical four-point bending strain gauge

Two sets of half-bridge tests were implemented by the symmetrical four-point bending method. The strain gauges were connected to the bridge box and the bridge box was connected to the YD-28A dynamic strain gauge, which was connected to the AdCras signal analysis system. The specimens were positioned on the supports as shown in Fig. 5, and the auxiliary beam was placed so that the loading point was located above the center of the 0° strain gauges. A total of 2.55 kg of weights were placed on the auxiliary beam three times for LVL and SPF plates and 0.85 kg of weights were placed on the auxiliary beam three times for straw plates to apply the load to the four-point bending system, and the strain values of the specimens were recorded using the software after each placement of the weights. Subsequent calculations were then performed.

## Asymmetric four-point bending method

The asymmetric four-point bending beam method for testing the shear modulus of wood is based on Shear Hooke's law and the equation for calculating the maximum shear stress at the point on the neutral axis of a rectangular section beam. The shear modulus is deduced by measuring the shear strain at the point on the neutral axis.

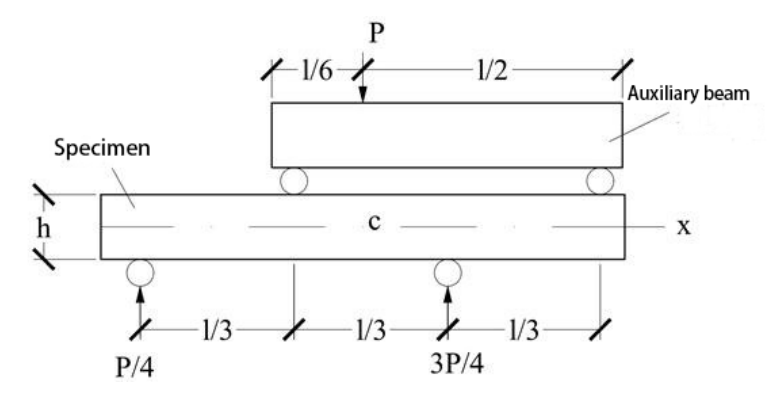


Fig. 6. Schematic diagram of the asymmetrically loaded four-point bending beam test setup

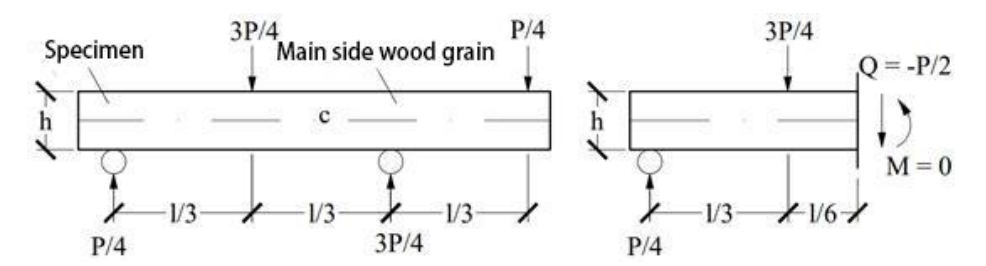


Fig. 7. Force diagram of asymmetrically loaded four-point bending beam

Because the shear stress at the point on the neutral axis of the cross-section of the beam is  $\tau_{max} = \frac{3Q}{2bh}$ , the shear stress at the center point of the side surface of the beam is  $\tau = \frac{3P}{4bh}$ , and the shear strain at the center point of the side surface of the beam is  $\gamma = \varepsilon_{-45^{\circ}} - \varepsilon_{45^{\circ}}$ .

According to the shear Hooke's law, the shear modulus G can be tabulated as  $G = \frac{3P}{4bh|\varepsilon_{-45^{\circ}} - \varepsilon_{45^{\circ}}|}$ , written in an incremental form that is easy to test as Eq. 6,

$$G = \frac{3\Delta P}{4bh|\Delta\varepsilon_{-45^{\circ}} - \Delta\varepsilon_{45^{\circ}}|} \tag{6}$$

where G is the shear modulus (MPa), b is the beam width (mm), h is the beam thickness (mm),  $\Delta P$  is the load increment (N),  $\Delta \varepsilon_{-45^{\circ}}$  and  $\Delta \varepsilon_{45^{\circ}}$  are the linear strains in the direction of negative 45° and positive 45° at the center point on the side of the beam, respectively, and  $|\Delta \varepsilon_{-45^{\circ}} - \Delta \varepsilon_{45^{\circ}}| = 2\varepsilon_{reading}$ .

If the full bridge method is used, Eq. 7 can be written as,

$$G = \frac{3\Delta P}{8bh\Delta\varepsilon_{reading}} \tag{7}$$

where  $\Delta \varepsilon_{reading}$  is the strain increment reading for full bridge measurement.

A 45° strain gauge was attached at the center points of the front and rear side surfaces of the beam specimen, as shown in Fig. 8. The beam was subjected to an asymmetric four-point bending load (Fig. 7), and the shear strain at the center point C was measured. The +45° and -45° strain gauges on the front and rear lateral surfaces of the beam were connected according to the full-bridge method, occupying one channel of the strain gauge.

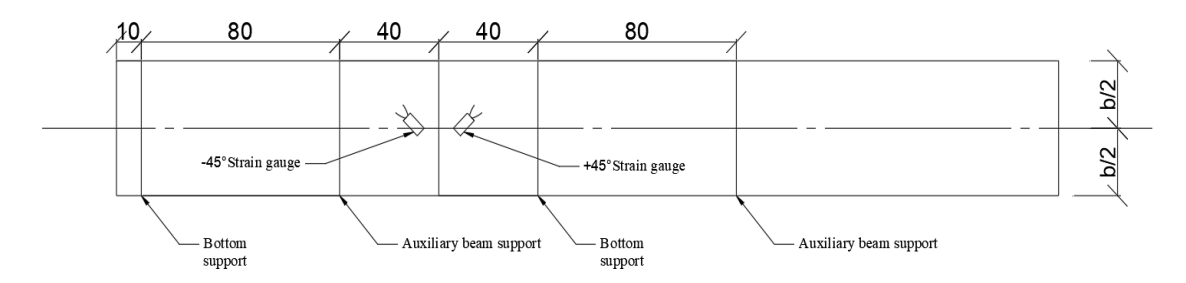


Fig. 8. Beam surface side (main directional surface) center point paste 45° strain gauge

The asymmetric four-point bending method was implemented for full-bridge testing by connecting the strain gauges to the bridge box and connecting the bridge box to the YD-28A dynamic strain gauge, which was connected to the AdCras signal analysis system. The specimen was positioned on the support as shown in Fig. 8, and the auxiliary beam was placed so that the loading point was  $\pm$  45° above the center of the strain gage. A 2.55 kg weight was placed on the auxiliary beam three times to apply the load to the four-point bending system, and the software was used to record the strain value of the specimen after each placement of the weight for subsequent calculations.

## **RESULTS AND DISCUSSION**

The results and analysis of the modulus of elasticity *E* and shear modulus *G* of the straw, LVL, and SPF panels measured by the transient excitation method and the four-point bending method described above were as follows.

# Test Results and Analysis of Rubber Belt Stiffness Coefficient k

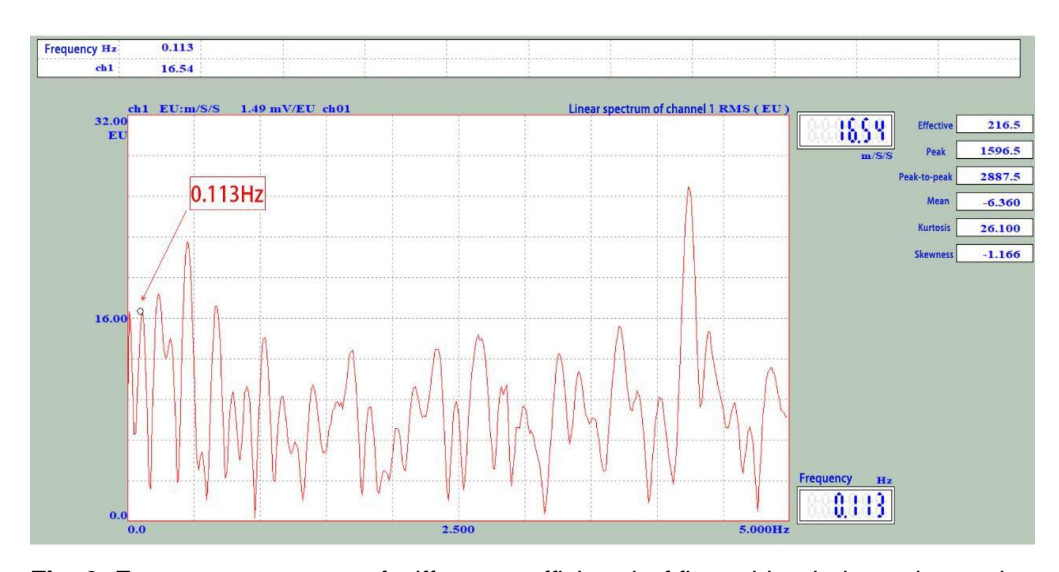
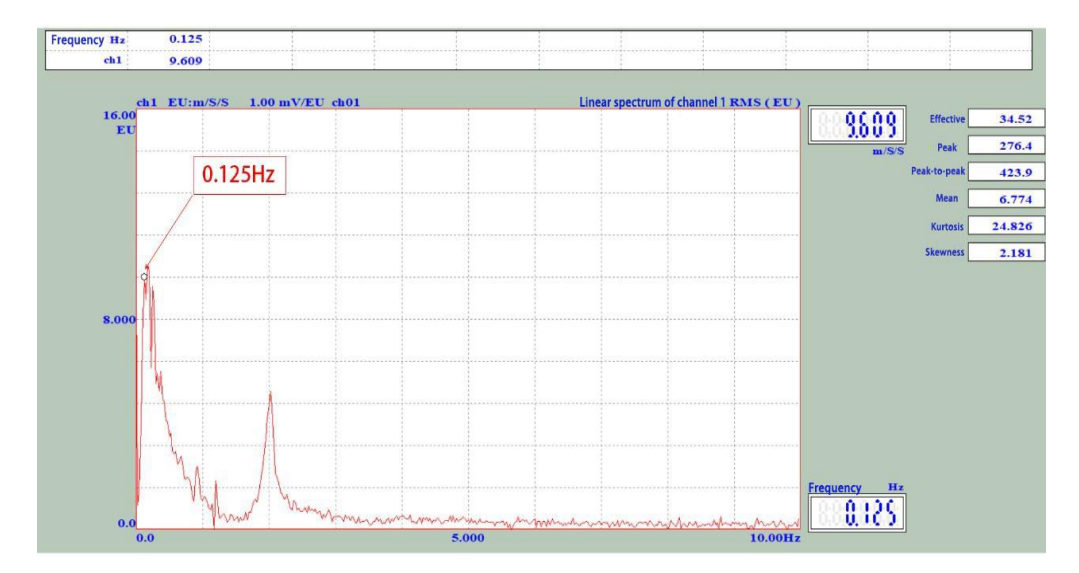


Fig. 9. Frequency spectrum of stiffness coefficient k of fine rubber belts and straw board



**Fig. 10.** Spectrum of stiffness coefficient *k* of medium rubber belt and LVL plate

As shown in Fig. 9, the fine rubber belts f under the JZ-1 plate specimen was determined to be 0.113 Hz. As shown in Fig. 10, the medium rubber belts f under the LZ-1 plate specimen was 0.125 Hz. Figure 11 shows that the coarse rubber belts f under the S-1 plate specimen was 0.150 Hz.

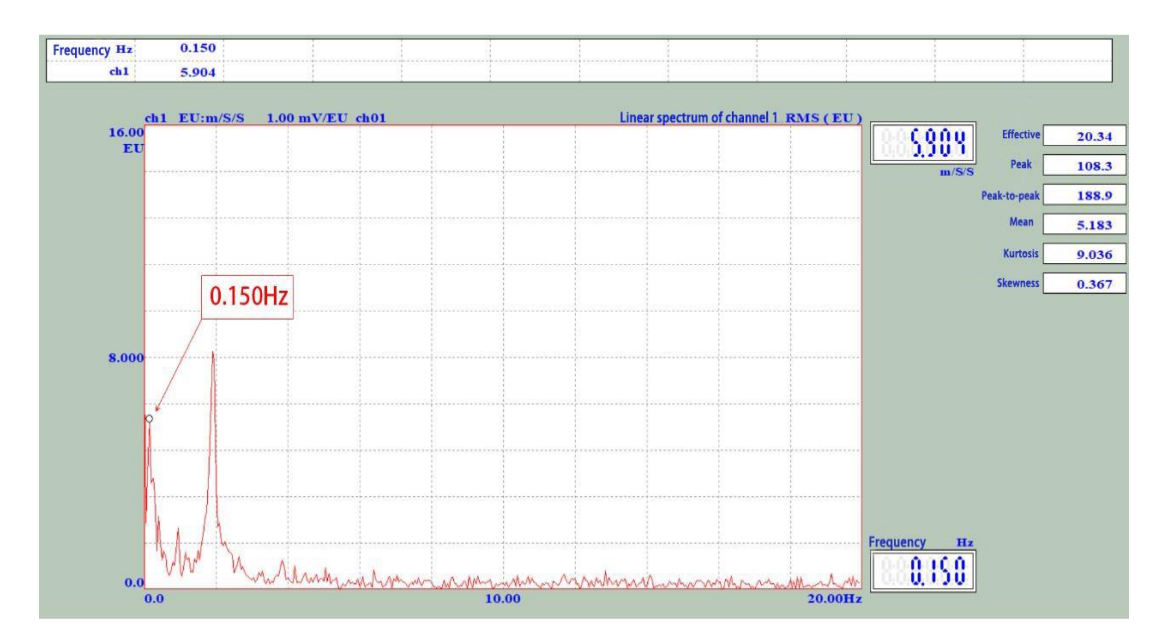


Fig. 11. Spectrum of coarse rubber belts and SPF plate stiffness coefficient k

Under the same straw board, the rigidity coefficient of three different sizes of rubber belts gradually increased with the thickness of the rubber belts, substituting the above f into Eq. 3 to obtain k, as shown in Table 2.

Name	Fine Rubber Belt <i>k</i> (N/m)	Medium Rubber Belt <i>k</i> (N/m)	Coarse Rubber Belt <i>k</i> (N/m)
Horizontal Straw Board	0.12	0.19	0.28
Longitudinal Straw Board	0.12	0.19	0.29
Horizontal LVL Panels	0.06	0.09	0.13
Longitudinal LVL Panels	0.06	0.09	0.14
Stringwise SPF Plate	0.05	0.07	0.10

Table 2. Effect of Different Types of Rubber Belts on k

It is known from Table 2 that the k-values ranged from 0.05 to 0.12 N/m under the action of the same fine rubber belts, from 0.07 to 0.19 N/m under the action of the same medium rubber belts, and from 0.10 to 0.28 N/m under the action of the same coarse rubber belts. The coarser the rubber belts were, the greater was its intrinsic frequency and the greater the  $\omega$  in Eq. 1 under the action of the same plate, *i.e.* the greater the rigidity coefficient k. The effect on its modulus of elasticity is very small, and the error range is negligible within 0.5%.

# Free Board Transient Excitation Test Results and Analysis

The straw board plate specimens were suspended to their vibration spectrum as shown in Fig. 12. The first-order bending frequency and first-order torsion frequency were identified and brought into the Eqs. 5, 6 to calculate the elastic modulus *E* and shear modulus *G* of the plate specimen. Figure 12 shows that the first-order bending frequency of the straw board JH-2 specimen was 217.5 Hz and the first-order torsion frequency was 662.5 Hz.

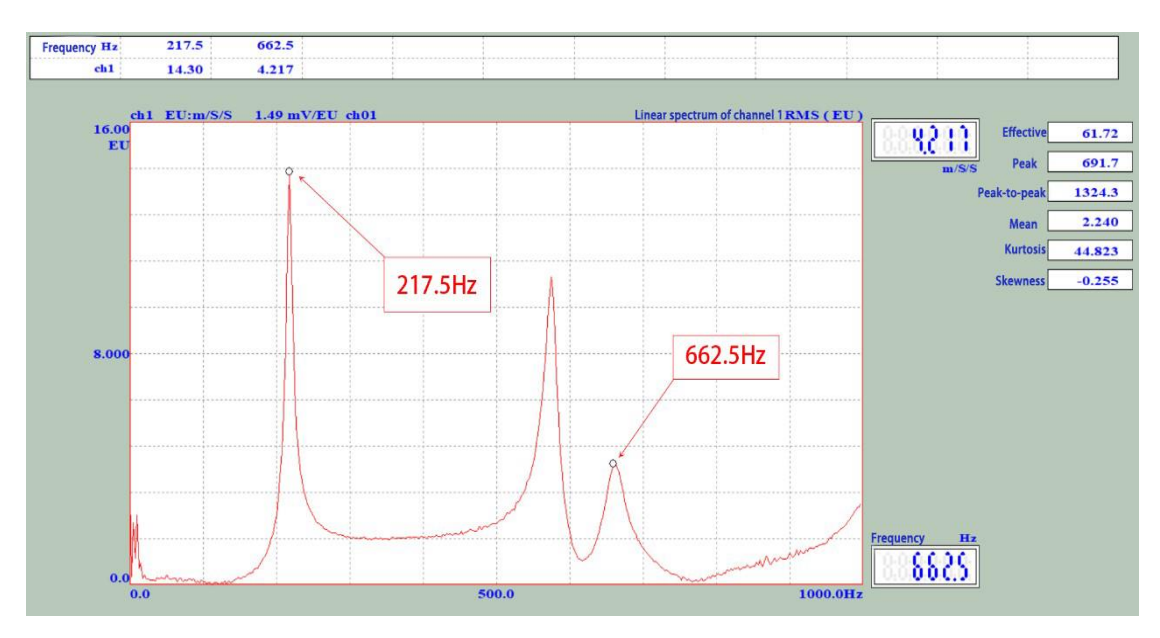


Fig. 12. Spectrum of straw board JH-2 specimen

**Table 3.** Test Results of Free Transient Excitation Plate Specimen E Suspended by Different Rubber Belts

Name	Mean Dynamic Elastic Modulus of the Thin Belts <i>E</i>	Mean Dynamic Elastic Modulus of the Thin Belts <i>E</i>	Mean Dynamic Elastic Modulus of the Thin Belts <i>E</i>	Mean Dynamic Elastic Modulus E	Error
Horizontal Straw Board	2836 (2.1%)	2864 (2.7%)	2864 (2.7%)	2854	0.9%
Longitudinal Straw Board	2319 (1.1%)	2329 (1.3%)	2338 (1.9%)	2329	0.4%
Horizontal LVL Panels	419 (8.5%)	476 (8.1%)	514 (7.3%)	470	7.9%
Longitudinal LVL Panels	10189 (1.0%)	10356 (1.5%)	11415 (1.8%)	10653	1.6%
Stringwise SPF Plate	11086 (3.3%)	11134 (3.3%)	11193 (3.3%)	11138	0.4%

Note: The numbers in parentheses are coefficients of variation.

As shown in Table 3, the coefficients of variation of dynamic elastic modulus E of straw board tested by fine, medium, and coarse rubber belts were all within 2.7%, and the error was within 0.9%; the coefficients of variation of dynamic elastic modulus E of LVL board tested by fine, medium, and coarse rubber belts were all within 8.5%, and the error was within 7.9%; the dynamic elastic modulus E of SPF board tested by fine, medium, and coarse rubber belts were all within 3.3%, and the error was within 1.6%. The coefficient of variation of dynamic modulus of elasticity E tested by three types of rubber tapes, namely, fine, medium, and coarse, was within 3.3%, and the error was within 1.6%.

**Table 4.** Test Results of Free Transient Excitation Plate Specimen G Suspended by Different Rubber Belts

Name	Mean Shear Modulus of Thin Belts G	Mean Shear Modulus of Middle Belts <i>G</i>	Mean Shear Modulus of Coarse Belts G	Mean Shear Modulus <i>G</i>	Error
Horizontal Straw Board	736 (2.9%)	747 (2.7%)	745 (2.9%)	743	1.4%
Longitudinal Straw Board	694 (1.1%)	701 (1.3%)	703 (1.3%)	699	0.9%
Horizontal LVL Panels	409 (2.1%)	455 (2.2%)	481 (1.9%)	448	5.7%
Longitudinal LVL Panels	749 (2.6%)	751 (2.5%)	776 (1.9%)	759	3.3%
String Wise SPF Plate	630 (7.4%)	638 (7.2%)	645 (7.5%)	638	1.1%

As shown in Table 4, the coefficient of variation of dynamic shear modulus G of straw board tested by fine, medium, and coarse rubber belts was within 2.9%, and the error was within 1.4%; the coefficient of variation of dynamic shear modulus G of LVL board tested by fine, medium, and coarse rubber belts were within 2.6%, and the error was within 5.7%; the dynamic shear modulus G of SPF board tested by fine, medium, and coarse rubber belts was within 7.5%, and the error was within 1.1%. The coefficient of variation of the dynamic shear modulus G of SPF plates tested by three types of rubber tapes, namely fine, medium, and coarse, was within 7.5%, and the error was within 1.1%.

# Free Beam Test Results and Analysis

To verify the correctness of the above material dynamic test results, the above five types of plate specimens were sawn into beam specimens, and their test results are shown in Table 5.

 Table 5. Specification and Number of Specimens for Each Beam

Name	Direction	Size Specification (mm × mm × mm)	Number	Quantity (Piece)
Ctrow Doord	Horizontal	420 × 18 × 18	JHL	3
Straw Board	Vertical	420 × 18 × 18	JZL	3
IVI Doord	Horizontal	384 × 16 × 16	LHL	3
LVL Board	Vertical	384 × 16 × 16	LZL	3
SPF Board	Chordwise	384 × 16 × 16	SL	3

**Table 6.** Modulus of Elasticity *E* for Plate and Beam Specimens

Name	Average Elastic Modulus of Plate <i>E</i> (MPa)	Average Elastic Modulus of Beam <i>E</i> (MPa)	Error (%)
Horizontal Straw Board	2864(2.7%)	2716(1.1%)	5.0
Longitudinal Straw Board	2329(1.3%)	2218(2.0%)	4.7
Horizontal LVL Panels	462(6.2%)	511(9.6%)	9.5
Longitudinal LVL Panels	10426(1.5%)	10802(4.6%)	3.4
String Wise SPF Plate	11134(3.3%)	10833(3.8%)	2.7

As shown in Table 6, the coefficients of variation of the dynamic elastic modulus E of the straw board plate specimens and the static elastic modulus E of the beam specimens were all within 2.7% and the error was within 5.1%. The coefficients of variation of the dynamic elastic modulus E of the LVL transverse plate specimens and the static elastic modulus E of the beam specimens were all within 9.6% and the error was within 9.5%, the dynamic elastic modulus of the LVL longitudinal plate and the coefficients of variation of dynamic modulus of elasticity E of beam specimens were within 4.6% and the error was within 3.4%. The coefficients of variation of dynamic modulus of elasticity E of SPF plate specimens and static modulus of elasticity E of beam specimens were within 3.8% and the error rate was within 2.7%.

**Table 7.** Beam Specimen Shear Modulus G

Name	Plate Shear Modulus G (MPa)	Beam Shear Modulus <i>G</i> (MPa)	Error (%)
Horizontal Straw Board	743(0.8%)	806(5.2%)	7.8
Longitudinal Straw Board	699(0.7%)	771(1.4%)	9.3
Horizontal LVL Panels	468(6.1%)	504(3.7%)	7.1
Longitudinal LVL Panels	759(2.0%)	821(7.9%)	7.5
String Wise SPF Plate	638(1.2%)	708(5.6%)	9.8

As shown in Table 7, the coefficients of variation of dynamic shear modulus G of the straw board panel specimen and static shear modulus G of the beam specimen were within 5.2%, and the error was within 9.3%; the coefficients of variation of dynamic shear modulus G of the LVL panel specimen and static shear modulus G of the beam specimen were within 7.9, and the error rate was within 7.5%; the coefficients of variation of dynamic shear modulus G of the SPF panel specimen and static shear modulus G of the beam

specimen were within 5.6%, and the error rate was within 9.8%. The coefficients of variation of dynamic shear modulus G of SPF plate specimens and static shear modulus G of beam specimens were within 5.6%, and the error was within 9.8%.

In summary, the correctness of the dynamic free-plate suspension transient excitation test was verified by the static four-point bending test with good reliability. The error levels of the elastic modulus E and shear modulus G of the same plate measured using three different thicknesses of rubber belts were less than 9.5% and 9.8%, respectively.

### CONCLUSIONS

- 1. When the elastic modulus E and shear modulus G of wood and its solid wood composite were tested dynamically by free board, the stiffness coefficient k of the suitable rubber strip ranged from 0.05 to 0.28 N/m. The k values of thin, medium, and coarse rubber belts selected in this study were 0.05 to 0.12N/m, 0.07 to 0.19N/m, and 0.10 to 0.28N/m, respectively.
- 2. The correctness and reliability of the dynamic freeboard suspension transient excitation test was verified by the static four-point bending test.
- 3. The error levels of the modulus of elasticity *E* and shear modulus *G* of the same sheet measured using three different thicknesses of rubber belts were less than 9.5% and 9.8%.

Rubber belts are mainly used to achieve free constraints on specimens, rather than directly participating in load transfer. During the testing process, rubber belts are usually arranged at specific angles to ensure that the specimen is properly restrained without lateral displacement. Rubber belts are intended to maintain deformation in the direction of applied pressure rather than lateral deformation (perpendicular direction to the applied pressure), and their elastic modulus is a more critical parameter in this case, which is crucial for maintaining the constraint of the specimen and determining the magnitude and direction of the force applied by the rubber belt to the specimen.

In addition, the shear deformation of rubber belts is relatively small, so their shear modulus has a relatively small impact on the test results. During the testing process, the rubber belt showed almost no trend of lateral displacement, further reducing the importance of shear modulus. The elastic modulus and shear modulus of the specimen are more influenced by the material properties of the specimen itself, rather than the performance of the rubber belt. Therefore, it is more important to ensure that the free constraints of the specimen are well achieved, rather than overly focusing on the material properties of the rubber belt. In this case, the elastic modulus and shear modulus of the rubber belt are not key parameters in the test.

### **Conflicts of Interest**

The authors declare that they have no known competing financial interests or personal relationships that could have appeared to influence the work reported in this paper.

## REFERENCES CITED

- ASTM D3044-16 (2016). "Test method for shear modulus of wood-based structural panels," ASTM International, West Conshohocken, PA, USA.
- Dauletbek, A., Li, H. T., Xiong, Z. H., and Lorenzo, R. (2021). "A review of mechanical behavior of structural laminated bamboo lumber," *Sustainable Structures* 1(1), article 000004. DOI: 10.54113/j.sust.2021.000004
- Hu, Y. C., Wang, F. H., Liu, Y. X., and, T Nakao (2001). "Detection of flexural modulus of elasticity of plywood by vibration method," *Wood Industry*. DOI: 10.19455/j.mcgy.2001.02.001
- Liu, J. M., Kong, X. H., Wang, C. J., and Yang, X. J. (2023a). "Permeability of wood impregnated with polyethylene wax emulsion in vacuum," *Polymer* 281, 1-8. DOI: 10.1016/j.polymer.2023.126123
- Liu, J. M., Wang, C. J., Yang, X. J., Bai, X. C., Tan, Y. J., and Kong, X. H. (2023b). "Interlaminar shear properties of glulam made of heat-treated laminates," *European Journal of Wood and Wood Products* 81, 887-896. DOI:10.1007/s00107-023-01934-7
- Mei, C. T., Zhou, G., and Zhang, Y. (2005). "Trial production of straw packing mat," *Forest Industry* 32(1), 36-38. DOI: 10.19531/j.issn1001-5299.2005.01.010
- Peng, Y. B., Wang, Z. H., and AI, X. Q. (2018). "Wind-induced fragility assessment of urban trees with structural uncertainties," *Wind & Structures* 26(1), 45-56. DOI: 10.12989/was.2018.26.1.045
- Quintero, M. A. M., Tam, C. P. T., and Li, H. T. (2022). "Structural analysis of a Guadua bamboo bridge in Colombia," *Sustainable Structures* 2(2), article 000020. DOI: 10.54113/j.sust.2022.000020
- Su, J. W., Li, H. T., Xiong, Z. H., and Lorenzo, R. (2021). "Structural design and construction of an office building with laminated bamboo lumber," *Sustainable Structures* 1(2), article 000010. DOI: 10.54113/j.sust.2021.000010
- Wang, Z. H., Wang, Z., Wang, B. J., Wang, Y. L., Rao, X., Liu, B., Wei, P. X., and Yang, Y. (2014). "Dynamic testing and evaluation of modulus of elasticity (MOE) of SPF dimension lumber," *BioResources* 9(3), 3869-3882. DOI: 10.15376/biores.9.3.3869-3882
- Wang, Z. H., Gao, Z. Z., Wang, Y. L., Cao, Y., Wang, G. G., Liu, B. and Wang, Z., (2015). "A new dynamic testing method for elastic, shear modulus and Poisson's ratio of concrete," *Construction and Building Materials* 100, 129-135. DOI: 10.1016/j.conbuildmat.2015.09.060
- Wang, Z. H., Wang, Y. L., Cao, Y., and Wang Z. (2016). "Measurement of shear modulus of materials based on the torsional mode of cantilever plate," *Construction and Building Materials* 124, 1059-1071. DOI: 10.1016/j.conbuildmat.2016.08.104
- Wang, Z., Xie, W. B., Wang, Z. H., and Cao, Y. (2018). "Strain method for synchronous dynamic measurement of elastic, shear modulus and Poisson's ratio of wood and wood composites," *Construction and Building Materials* 182, 608-619. DOI: 10.1016/j.conbuildmat.2018.06.139
- Wang, Z., Xie, W. B., Lu, Y., Li, H. T., and Wang, Z. H. (2019). "Dynamic and static testing methods for shear modulus of oriented strand board," *Construction and Building Materials* 216, 542-551. DOI: 10.1016/j.conbuildmat.2019.05.004
- Wang, Z. H., and Ghanem, R. (2021). "An extended polynomial chaos expansion for PDF characterization and variation with aleatory and epistemic uncertainties,"

- Computer Methods in Applied Mechanics and Engineering 382, article ID 113854. DOI: 10.1016/j.cma.2021.113854
- Wang, Z. H., and Ghanem, R. (2022). "A functional global sensitivity measure and efficient reliability sensitive-ty analysis with respect to statistical parameters," *Computer Methods in Applied Mechanics and Engineering* (Available Online), article ID 115175.
- Wang, Z. H., and Ghanem, R. (2023a). "Stochastic modeling and statistical calibration with model error and scarce data," *Computer Methods in Applied Mechanics and Engineering* 416, 116339. DOI:10.1016/j.cma.2023.116339
- Wang, Z. H., and Ghanem, R. (2023b). "Stochastic framework for optimal control of planetary reentry trajectories under multilevel uncertainties," *AIAA Journal* 61(8), 3257-3268. DOI:10.2514/1.J062515
- Wang, Z. H., Hawi, P., Masri, S., Aitharaju, V., and Ghanem, R. (2023). "Stochastic multiscale modeling for quantifying statistical and model errors with application to composite materials," *Reliability Engineering and System Safety* 235, 109213. DOI:10.1016/j.ress.2023.109213
- Yin, S. C. (1996). *Timber Science*, China Forestry Press, Beijing, China. Zhang, X. Y. (2015). *University Physics*, Higher Education Press, Beijing, China.
- Zhou, Y. H., Huang, Y. J., Sayed, U., and Wang, Z. (2021). "Research on dynamic characteristics test of wooden floor structure for gymnasium," *Sustainable Structures* 1(1), article ID 000005. DOI: 10.54113/j.sust.2021.000005

Article submitted: March 10, 2024; Peer review completed: April 24, 2024; Revised version received: May 12, 2024; Accepted: September 8, 2024; Published: September 23, 2024.

DOI: 10.15376/biores.19.4.8512-8526